PHYSICAL REVIEW A VOLUME 19, NUMBER 4 APRIL 1979

Integrability of multiple three-wave interactions

James D. Meiss
Department of Physics, University of California, Berkeley, California 94720
(Received 25 September 1978)

Numerical evidence is presented which indicates that the N-degree-of-freedom Hamiltonian that describes a set of pairs of sinusoidal waves interacting with a single, "test" wave is completely integrable. Computations of the Poincaré surface of section and Greene's residues provide the evidence for two background wave pairs. Linear separation of neighboring orbits for up to four wave pairs also suggests integrability for more degrees of freedom.

I. INTRODUCTION

In this paper we discuss numerical evidence for complete integrability of a physically interesting, N-degree-of-freedom Hamiltonian. The dynamical system, introduced in Sec. II, consists of a set of waves interacting in groups of three. One member of each triad is a particular wave denoted the "test wave." Thus the Hamiltonian describes the evolution of the test wave upon interaction with a spectrum of background waves.

It is well known that the equations of motion for a one-degree-of-freedom conservative system can be integrated using the constancy of the energy. However, for systems with more than one degree of freedom, integrability is exceptional—requiring the existence of additional integrals of motion. More precisely, an N-degree-of-freedom system is integrable if there exist N isolating integrals in involution.[1] The difficulty of finding these integrals is indicated by the small number of known integrable systems. Those of physical interest include the Toda[2,3] and Calogero-Moser[4] lattices. Moreover, theorems by Siegel[5] indicate that nonintegrability is probable for a large class of Hamiltonians.

While the existence of N integrals for a completely integrable system restricts the region in phase space that is traversed by any trajectory to an N-dimensional surface, an orbit in a nonintegrable system does not have this restriction. For Hamiltonians of this type a single orbit may densely fill a higher-dimensional region in the phase space. This type of motion, termed "stochastic," has been observed numerically for many systems (e.g., Hénon and Heiles[6]).

Even though it is possible to numerically demonstrate nonintegrability,[7] we have been unable to find evidence of stochastic behavior for our system. In lieu of the discovery of the integrals for the test-wave system, we have constructed several numerical tests which indicate integrability (or at least lack of stochasticity).

The test-wave Hamiltonian is introduced in Sec. II, and several general characteristics of the system are discussed. Section III consists of a brief discussion of the well-known, single-triad case. In Sec. IV we construct the Poincaré surface of section mapping.[8] We apply this to the two-degree-of-freedom case, for which the surface is a plane. The regularity of this mapping (Fig. 4) is an indication of integrability. In Sec. V we examine the separation of nearby orbits as a function of time.[8] For every pair of orbits we tested for the two-, three-, and four-degree-of-freedom systems, the separation was not exponentially increasing in time; thus this system does not exhibit the instability characteristic of a C system.[9] The absence of this local stochastic behavior indicates integrability. Finally in Sec. VI we apply the most sensitive, yet least known, test: Greene's residue method.[10,11] With this method we probe the fine structure of the surface of section constructed in Sec. IV by considering the linearization of the mapping near periodic points. With this we can show quantitatively that the surface of section mapping is indeed regular as it appears in Fig. 4.

II. TEST-WAVE HAMILTONIAN SYSTEM

Our Hamiltonian (1) describes a weakly nonlinear physical system[12] consisting of interacting waves. In the linear approximation the system is composed of a superposition of uncoupled sinusoidal waves or equivalently—harmonic oscillators. The lowest-order nonlinearity (the only one considered here) couples the waves in triads with coupling strength proportional to the product of the wave amplitudes. Examples of such systems include lattice vibrations, sound waves, plasma waves, and water waves.

As a simplification to the dynamics we consider only interactions involving a single labeled wave. Triads containing only the remaining, background waves are neglected. Energy transfer among the background waves is therefore accomplished only

through the mediation of the labeled or test wave.

Test-wave dynamics have been studied for the ocean with coupling between surface and internal waves.[13] In this model a single internal wave is coupled to a spectrum of surface waves. Since the lowest-order resonant interaction among surface waves is the four-wave interaction, the neglect of interactions among the background is a consistent approximation to third order. The test-wave model also applies to the generation of a transverse plasma wave through interaction with pairs of longitudinal waves,[14] and to two-dimensional turbulence (here the unperturbed wave frequencies are zero).[15] Our own interest in the model is for interactions among oceanic internal waves.

We introduce the Hamiltonian in terms of action-angle variables. These are convenient variables to use for analytical purposes since the actions are constant for the unperturbed system. The test-wave action is designated J_0 and the background wave actions are $\{J_n, J_n' | n=1, M\}$. The Hamiltonian is

$$H=\omega_0 J_0+\sum_{n=1}^{M}(\omega_n J_n+\omega_n' J_n') - \sum_{n=1}^{M}\epsilon_n(J_0 J_n J_n')^{1/2}\cos(\theta_n-\theta_n'-\theta_0). \tag{1}$$

Here the ω_i are the linear wave frequencies, the θ_i are the wave phases, and the ϵ_i represent the coupling coefficients. The system has $2M+1$ degrees of freedom. Note that the background wave J_i directly interacts only with the wave J_i' and the test wave.

Action variables, however, are not useful for numerical integration of the equations of motion since these equations are singular at $J=0$. Instead we use the action-amplitude coordinates[12] for computations:

$$a_k\equiv(2J_k)^{1/2}e^{-i\theta_k}=q_k+ip_k, \quad k=1,2,\ldots,2M+1. \tag{2}$$

In terms of the action amplitudes a_i or the canonical rectangular coordinates (q_i, p_i), the Hamiltonian is a cubic polynomial and the equations of motion have no singularities.

Since the phases occur in only M independent combinations in (1), we can define a canonical transformation to a new system with only M degrees of freedom. Following the notation of Goldstein,[16] the generating function for this transformation is

$$F_2=I_0\theta_0+\sum_{n=1}^{M}I_n(\theta_n-\theta_n'-\theta_0)+\sum_{n=1}^{M}I_n'\theta_n'. \tag{3}$$

The new coordinates I, ψ can be expressed in terms of the old as

$$I_n=J_n, \quad I_n'=J_n'+J_n, \quad I_0=J_0+\sum_{i=1}^{M}J_i, \quad \psi_n=\theta_n-\theta_n'-\theta_0, \tag{4}$$

where

$$n=1,2,\ldots,M.$$

For the new Hamiltonian we find (up to an additive constant)

$$K=\sum_{n=1}^{M}\Delta_n I_n-\sum_{n=1}^{M}\epsilon_n V_n\cos\psi_n, \quad \Delta_n\equiv\omega_n-\omega_n'-\omega_0, \quad V_n\equiv\left[I_n(I_n'-I_n)\left(I_0-\sum_{I=1}^{M}I_I\right)\right]^{1/2}. \tag{5}$$

From the equations of motion for (5) we see that the momenta I_n' and I_0 are constants and thus ignorable. The phase space of the new system is bounded by the requirement that the original actions be positive:

$$0\le I_n\le I_n', \quad \sum_{n=1}^{M}I_n\le I_0. \tag{6}$$

The energy is therefore also bounded.

The frequency differences Δ_n indicate the degree of resonance mismatch of the linear oscillators. $\Delta_n=0$ is called resonance because in the limit of no coupling ($\epsilon_n=0$) the phases ψ_n are constants. This corresponds to resonant locking of the three-wave phases which, for a finite but small ϵ_n, causes a large oscillation of the actions. As the mismatch increases the oscillation amplitudes of the actions decrease. In fact if one of the $\Delta_n \gg \epsilon_n\sqrt{I_n}$ then the corresponding action is essentially constant and its degree of freedom can be ignored. This will be seen more specifically for the single triad ($M=1$) case discussed in Sec. III.

An interesting consequence of the equations of motion for the test-wave system in exact resonance ($\Delta_n=0$) is a tendency for phase coherence among the modes. The most extreme example of this is an initial condition for which $\psi_n=\pm\frac{1}{2}\pi$; then all the phases will oscillate as "square waves" between $\frac{1}{2}\pi$ and $-\frac{1}{2}\pi$ with the same fundamental period. Similarly the actions oscillate together between zero and their maximum values. Also initial conditions with the actions at their respective extrema (6), regardless of the phases, yield square-wave oscillation of the phases. Examples of these trajectories are shown in Fig. 1 for the $M=2$ and 3 cases. The figure displays the actions I and the phases ψ as functions of time. Figures 1(a) and 1(b) are square-wave solutions for the

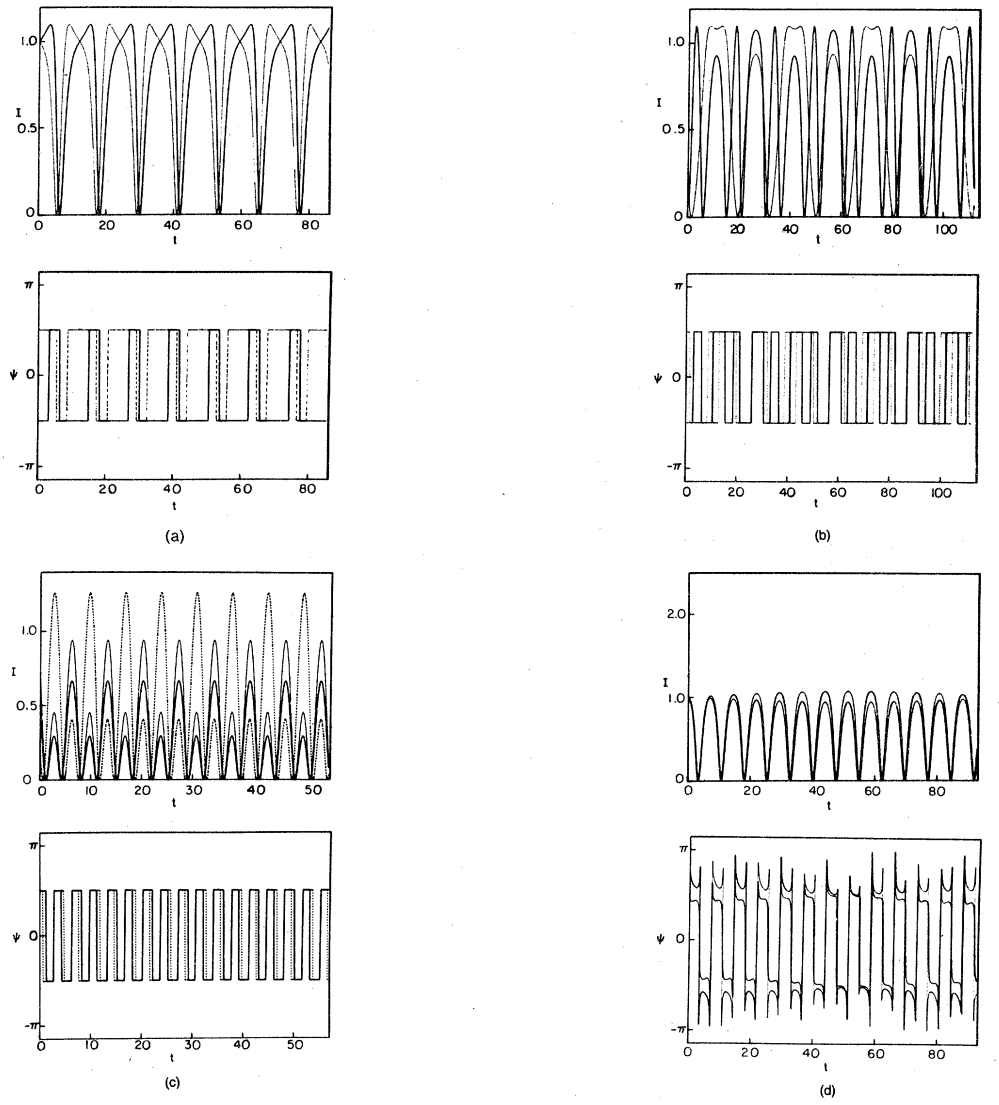

FIG. 1. Examples of square-wave trajectories for the $M=2$, 3 systems. In (a) and (b) $I_1'=I_2'=1.1$, $I_0=2.01$, $\epsilon_1=\epsilon_2=1$. I_1 and ψ_1 are shown by solid lines, I_2 and ψ_2 by dotted lines. For (c), $I_1'=1.1$, $I_2'=1.6$, $I_3'=1.9$, $I_0=2.01$, $\epsilon_n=1$, ψ_1 and ψ_2 are superimposed. In (d) the parameters are the same as for (a). This trajectory is *near* a square-wave trajectory since $\psi_1(0)\neq\pi/2$.

two-triad case with $I_1(0)=I_2(0)$; $\psi_1(0)=-\frac{1}{2}\pi$; $\psi_2(0)=\frac{1}{2}\pi$. Since $I_1'=I_2'$ for these figures the actions oscillate between the same absolute limits, as derived from (6). In Fig. 1(b) the second of Eqs. (6), $I_1+I_2\leq I_0$, further restricts the actions from being simultaneously large. Figure 1(c) is a three-triad computation for which the initial actions and the I_n' are not equal, but $\psi_n(0)=\frac{1}{2}\pi$. Further computations show that square-wave phase oscillations also occur for cases in which the ϵ_n are not equal. The Fig. 1(d) is a computation for the $M=2$ system with initial conditions near the square-wave case: $\psi_2(0)=\frac{1}{2}\pi$; $\psi_1(0)>\frac{1}{2}\pi$. The phases both oscillate between π and $-\pi$ but spend most of the time $\pm\frac{1}{2}\pi$. Discontinuities in the phase graph are due to restricting the phases to the range $(-\pi,\pi]$.

For the special case in which the I_n' are equal, the ϵ_n are equal, and the $I_n(0)$ are equal, the equations of motion can be easily integrated, for the square-wave case, yielding (see Sec. III)

$$I_n(t)=I_<\mathrm{sn}^2(\tfrac{1}{2}\epsilon(MI_>)^{1/2}t+\delta)$$

$$\psi_n(t)=\begin{cases}-\frac{1}{2}\pi, & \delta+jT<t<\delta+(j+\frac{1}{2})T,\\ +\frac{1}{2}\pi, & \delta+(j+\frac{1}{2})T<t<\delta+(j+1)T,\end{cases}$$

where $j=0,1,\ldots$.

$$T=\frac{4}{\epsilon}\frac{1}{(MI_>)^{1/2}}F(\tfrac{1}{2}\pi\,|\,I_</I_>),$$
$$I_<=\min(I',I_0/M), \tag{7}$$
$$I_>=\max(I',I_0/M).$$

Here sn is a Jacobi elliptic function and F is the elliptic integral of the first kind.[17] Thus the actions oscillate between zero and $I_<$ [the maximum possible according to Eq. (6)] with period T. In Fig. 2 this solution is displayed for the two-triad ($M=2$) system. Computations show that the qualitative behavior of all square-wave type trajectories is similar. A more general solution, also for $K=0$, has been obtained for a similar system by Wilhelmsson for the $M=2$ case.[14]

While the values $\pm\frac{1}{2}\pi$ for the phases yield large oscillations for the resonant system there are 2^M distinct equilibrium points in phase space given by

$$\psi_n=0 \text{ or } \pi,$$
$$\sum_{n=1}^{M}\left(\epsilon_n\frac{\partial}{\partial I_n}V_n\right)\cos\psi_n=0. \tag{8}$$

Computations with orbits near these points show that the two points $\psi_n=0$ and $\psi_n=\pi$ are asymptotically stable (orbits remain close for all time) while the other points are "stable" only for a short time: nearby orbits begin as small oscillation, but the amplitude of the oscillation may grow in time. This latter motion is qualitatively similar to a particle near a saddle point in a potential well.

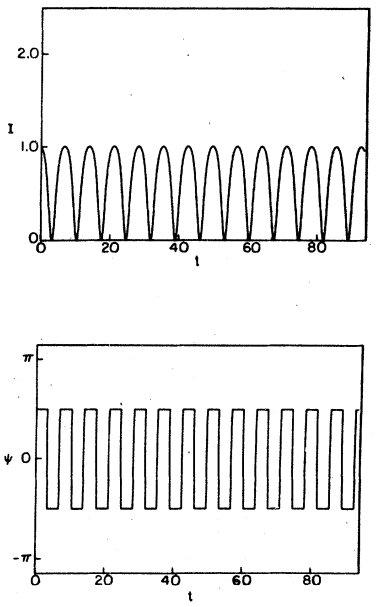

FIG. 2. Trajectory of Eq. (7). The parameters are the same as for Fig. 1(a).

III. SINGLE-TRIAD CASE

For the case $M=1$, a single-triad interaction, the Hamiltonian (5) has only one degree of freedom and can be easily explicitly integrated. This Hamiltonian has been studied numerous times[12,14,18-20] but for completeness we briefly summarize the results. A qualitative discussion of the phase space and the orbits is given in Ref. 12.

The equations of motion are

$$\dot{I}=-\epsilon V\sin\psi,\quad \dot{\psi}=\Delta_n-\epsilon\frac{\partial V}{\partial I}\cos\psi. \tag{9}$$

Upon squaring the first equation, the equation of motion for the action I becomes equivalent to that for a particle in a one-dimensional well with the potential energy

$$U=\tfrac{1}{2}\left[(K-\Delta I)^2-\epsilon^2 I(I'-I)(I_0-I)\right] \tag{10}$$

and total energy zero. The extrema of motion are given by the smallest two zeros of $U(I)$, which are real and non-negative for physical values of the parameters. We label the zeros as $\mathcal{I}_1$, $\mathcal{I}_2$, and $\mathcal{I}_3$ such that

$$0\leq\mathcal{I}_1\leq\mathcal{I}_2\leq\min(I',I_0)\leq\mathcal{I}_3. \tag{11}$$

The solution for the action is then

$$I(t)=\mathcal{I}_1+(\mathcal{I}_2-\mathcal{I}_1)\mathrm{sn}^2(\tfrac{1}{2}\epsilon(\mathcal{I}_3-\mathcal{I}_1)^{1/2}t-\delta) \tag{12}$$

with the oscillation period

$$T=\frac{4}{\epsilon}\frac{1}{(\mathcal{I}_3-\mathcal{I}_1)^{1/2}}F\left(\tfrac{1}{2}\pi\left|\frac{\mathcal{I}_2-\mathcal{I}_1}{\mathcal{I}_3-\mathcal{I}_1}\right.\right). \tag{13}$$

The square-wave solution is obtained by setting $\Delta=0, K=0$ for which $\mathcal{I}_1=0$, $\mathcal{I}_2=\min(I_0,I')$, and the oscillations are over the entire range of allowed variation of the action (6).

As Δ increases the amplitude of oscillation decreases. Figure 3 shows the maximum amplitude

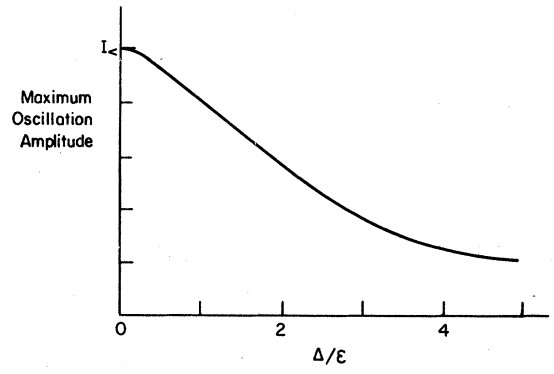

FIG. 3. Maximum oscillation amplitude as a function of resonance mismatch Δ for the single-triad case. Here $I_>/I_<=3$.

of oscillation as a function of Δ/ϵ for the particular choice $I_0/I' = 3$. The maximum oscillation amplitude occurs for an energy of approximately $\frac{1}{2}\Delta$. The width of the amplitude curve is $\Delta \simeq \epsilon\sqrt{I_0}$; therefore, if Δ is much larger than this the action is constant.

IV. POINCARE SURFACE OF SECTION

For the two-triad ($M = 2$) case the Hamiltonian (5) has two degrees of freedom, and integrability is no longer guaranteed. In this section we discuss the Poincaré surface of section for this system and show how it fails to indicate nonintegrability.

First we define the canonical rectangular coordinates corresponding to the transformed action-angle coordinates (I, ψ) by

$$p_i = -(2I_i)^{1/2}\sin\psi_i, \quad q_i = (2I_i)^{1/2}\cos\psi_i. \tag{14}$$

By constructing the Poincaré surface of section mapping we can qualitatively check for the existence of a second integral of motion, beyond the energy, for this system. To construct the mapping consider orbits confined to a particular three-dimensional energy surface defined by

$$K = K(p_1, q_1, p_2, q_2). \tag{15}$$

Our surface of section is essentially the intersection of this surface with the surface $p_2 = 0$. We may use (p_1, q_1) as coordinates of this surface since the value of q_2 is determined by solving (15) with $p_2 = 0$ upon choosing a particular branch. The relation $q_2(p_1, q_1; K)$ is double valued, the branches being distinguished by the sign of $\partial K/\partial q_2 = -\dot{p}_2$. We take $\dot{p}_2 > 0$ and denote the corresponding function as q_2^+. $\dot{p}_2 < 0$ yields similar results.

As a trajectory with the specified energy evolves in time it may repeatedly intersect the surface of section, now represented as a region of the p_1-q_1 plane defined implicitly by

$$K = K(p_1, q_1, p_2 = 0, q_2), \quad |q_2| < q_2^{\max}, \quad \dot{p}_2 > 0. \tag{16}$$

Successive intersection points uniquely define the Poincaré mapping on the plane. If no invariant exists besides the energy, then these intersection points will densely fill some area of the plane; however, if the invariant does exist then the intersection points must lie on a smooth level curve of this invariant. If the second integral C were known the equation of the level curves would be obtained by simply substituting the values of p_2 and q_2 on the surface of section into the form of the integral $C(p_1, q_1, p_2, q_2)$, yielding

$$C = C[p_1, q_1, p_2 = 0, q_2^+(p_1, q_1; K)]. \tag{17}$$

Thus the existence of level curves on all surfaces of section implies the existence of the invariant.

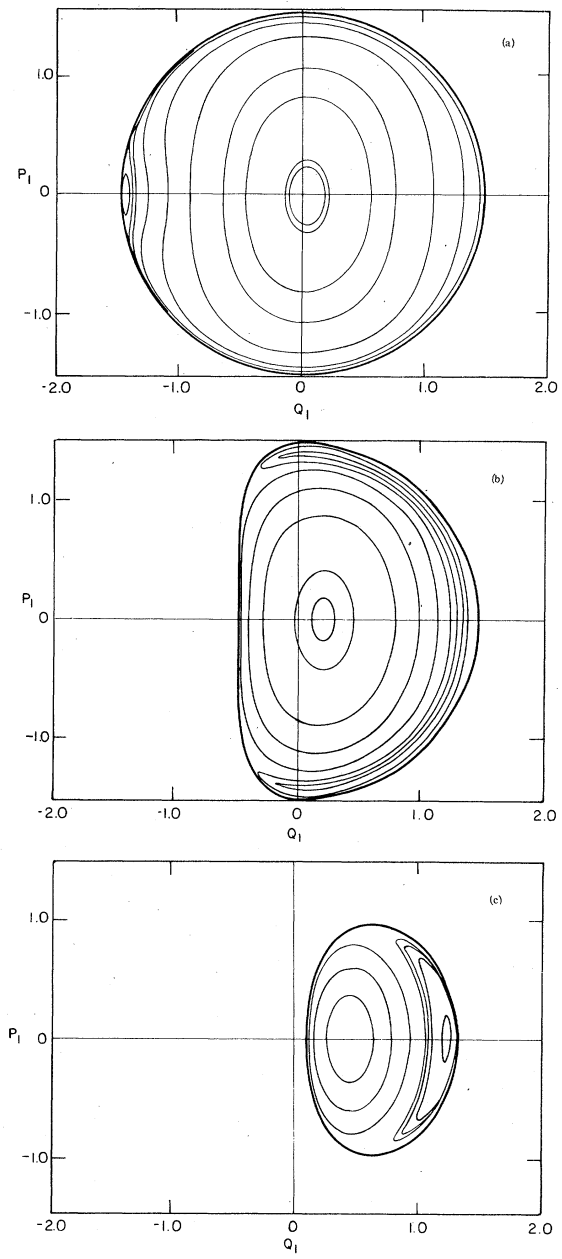

FIG. 4. Surfaces of section for $M = 2$; $I_1' = 1.1$; $I_2' = 1.6$; $I_0 = 2.01$; $\epsilon_1 = \epsilon_2 = 1$. The energies for (a), (b), and (c) are $K = -0.1$, -0.5, -1.0, respectively.

Computationally one must contend with a finite set of mapping iterates generated by the computer. It is thus impossible to be certain whether or not these points lie on a smooth curve. In practice, however, the distinction for many systems[6,8,21] is easily made because of a great difference in the complexity of nonstochastic and stochastic mappings. With these remarks we turn to the mapping for the test-wave system.

Typical surface of section plots for three values

of the energy are presented in Fig. 4, for the choice of parameters: $I_1' = 1.1, I_2' = 1.6, I_0 = 2.01$, $\epsilon_1 = \epsilon_2 = 1, \Delta_1 = \Delta_2 = 0$. For these parameters $|K| \leq 1.322$. Since the orbits are invariant under $\psi_n \to \psi_n + \pi, K \to -K$; we may consider one sign of the energy. Figure 4, therefore, represents a survey of the entire allowed range of energy. We have also numerically integrated the equations of motion for points chosen over the entire allowed region of the p_1-q_1 plane for each energy. The dark curves in Fig. 4 enclose this region. As the energy approaches -1.322 the surface of section shrinks to a point on the q_1 axis. This point is a stable equilibrium [see Eq. (8)].

The remaining curves in Fig. 4 are each generated by the repeated intersections with the plane of a single trajectory. A typical curve was drawn through 50 intersection points when the ordered, quasiperiodic nature of the mapping was clear. In each surface of section there are two elliptic fixed points which correspond to periodic orbits in the full phase space. Each of these fixed points is on the q_1 axis.

Smooth curves are present in the surface of section plots for other values of the parameters including nonequal ϵ_n and nonzero Δ_n. We have been unable to find any evidence of stochastic regions on any surface of section.

V. SEPARATION OF NEIGHBORING ORBITS

As another test for stochastic motion we compute the rate of separation of nearby trajectories. A pair of trajectories in a highly stochastic region of phase space will separate exponentially in time, while every nearby pair of trajectories for an integrable system will separate only linearly in time.

Exponential separation is a property of highly stochastic systems called C systems.[9] For a C system, phase space in the neighborhood of a trajectory can be decomposed into two subspaces. In one subspace every trajectory diverges exponentially from other trajectories as time increases; in the other, the trajectories converge. A randomly selected separation vector will have components in the dilating subspace that quickly overwhelm the contracting components; therefore most trajectories will diverge. One property of C systems is an extreme sensitivity of the flow to initial conditions since two trajectories initially infinitesimally separated will at a later time be a macroscopic distance apart. A C system is also ergodic and mixing on the energy surface.[9]

For an integrable system it is always possible to find a set of *true* action-angle coordinates $(\vec{\mathcal{J}}, \vec{\phi})$. In these coordinates the Hamiltonian is only a function of the action so that the solutions to the equations of motion are

$$\vec{\mathcal{J}}(t) = \vec{\mathcal{J}}(0), \quad \vec{\phi}(t) = \vec{\omega}(\vec{\mathcal{J}})t + \vec{\phi}(0). \tag{18}$$

Since the angle variables are periodic each orbit lies on an N-dimensional torus. In terms of these coordinates the rate of separation of two orbits is

$$\frac{d}{dt}(\vec{\phi}_1 - \vec{\phi}_2) = \vec{\omega}(\vec{\mathcal{J}}_1) - \vec{\omega}(\vec{\mathcal{J}}_2) \tag{19}$$

which is a constant, thus the distance increases linearly in time.

A "typical" nonintegrable system is not a C system, but seems to have regions in phase space of exponential orbit separation. These orbits usually correspond to those found to be stochastic by the methods of Secs. IV and VI. It is, however, possible for a system to be nonintegrable (even mixing and ergodic) and not exhibit C-system behavior.[22] Therefore a system with linearly separating orbits is not a C system, but it may also not be an integrable system.

The use of the exponential separation method is not restricted to systems of two degrees of freedom, as is the surface of section method, but like that method the results are qualitative. It is difficult to precisely distinguish between the two regimes in computations, because for small times an exponential curve is linear. Yet the computations cannot be continued too long or the boundaries of the phase space are encountered and growth of the distance must stop. We circumvent this restriction by initializing the orbits at a distance small compared to the size of the phase space.

We calculated the orbit separation for the systems $M = 2$, 3, and 4 and found that it was never exponential. To cover the phase space we chose several hundred initial conditions with the actions on a grid and the phases picked randomly. Typical separation curves are shown in Fig. 5, where we have plotted the logarithm (base 10) of the distance against time. Distance was calculated using the coordinates (2) with a Euclidean metric. Note, however, that the exponential-linear distinction is independent of the metric used (Ref. 9, p.55). At $t = 0$ the fractional separation between orbits was typically 10^{-7} in one of several directions. For Fig. 5(a) the initial separation is in an action (J) direction, while in Fig. 5(b) and 5(c) it is in an angle (θ) direction. The generally negative curvature of each of these curves is indicative of the nonexponential growth rate. The small oscillations on these curves have periods similar to those of the trajectories themselves. Oscillations of this sort are present in both integrable and nonintegrable systems, although generally seem to be more regular in integrable systems.

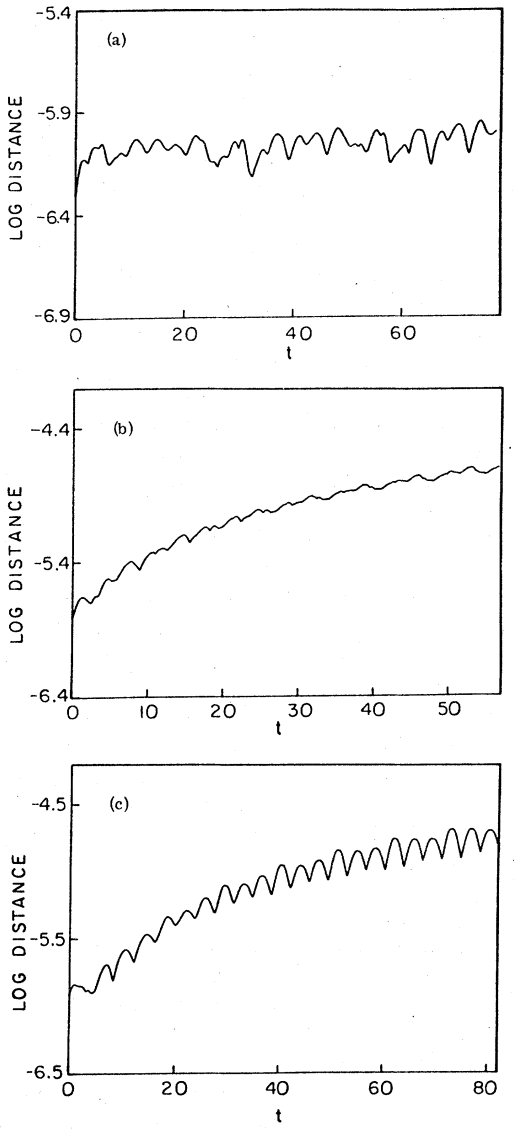

FIG. 5. Separation of nearby orbits as a function of time for $M=2$, 3. Log_{10} of the Euclidean distance is plotted. For (a) the initial separation was in the J direction, while for (b) and (c) it was in the θ direction.

Since the orbit separation for the test-wave system with up to four triads is linear, we are unable to find evidence of nonintegrability for this system. Since for up to four triads the orbits are qualitatively similar, the evidence tentatively indicates that the test-wave system with an arbitrary number of degrees of freedom is integrable.

VI. GREENE'S RESIDUES

The most sensitive integrability test is applicable only to systems with two degrees of freedom: the residue method of Greene.[10] Although this method is clearly explained in Greene's paper, it is apparently not widely known so we give a brief description of it.

Greene develops the method for plane, area-preserving mappings. For the case of a two-degree-of-freedom Hamiltonian, the surface of section discussed in Sec. IV is such a mapping [e.g., the $K=-0.1$ surface of section, Fig. 4(a)]. To apply the mapping to a point on the surface, integrate the equations of motion forward in time until the orbit again intersects the surface. Symbolically, we refer to this procedure as a nonlinear mapping T:

$$(p_1', q_1') = T(p_1, q_1). \tag{20}$$

On the $K=-0.1$ surface there are two first-order fixed points of this mapping, defined by

$$(p_1, q_1) = T(p_1, q_1). \tag{21}$$

For example, the central fixed point in Fig. 4(a) is at $q_1 = 0.03878, p_1 = 0.0$. These fixed points generally represent periodic orbits in the full phase space rather than equilibria. In Fig. 4(a) the fixed points are elliptic since iterations of the mapping for points nearby result in elliptical curves. The rotation number of a particular surface of section curve about the elliptic fixed point is defined as

$$\omega = (\text{average angle per mapping iteration})/2\pi. \tag{22}$$

For curves close to the fixed point $\omega = 0.46$. The rotation number is a monotonically decreasing function of radial distance from the fixed point, approaching zero at the separatrix (outermost orbit encircling the fixed point). For the fixed point discussed here this curve is shown in Fig.

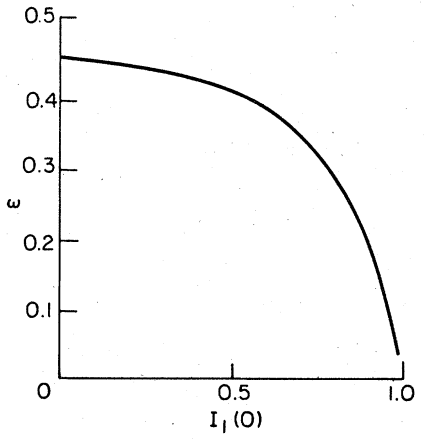

FIG. 6. Rotation number as a function of initial conditions. The parameters are the same as for Fig. 4 with $K=-0.1$. Initial conditions are $I_2 = 0.001$, $\psi_2 = 0$, with ψ_1 determined by I_1.

6. Here the value of I_1 is essentially the radial distance from the fixed point since this point is so close to the origin.

If the rotation number is irrational then the iterates of the mapping will fill a curve on the surface of section. If, however, the rotation number is rational, e.g., $\omega = P/Q$, then the mapping is periodic after Q iterations. A point with rotation number P/Q is a fixed point of the Qth power of the mapping T:

$$(p_f, q_f) = T^Q(p_f, q_f) . \tag{23}$$

Since the rotation number is a smooth function, there is an infinity of these higher-order fixed points.

Calculation of the residue determines the character of these fixed points. To define the residue, consider initial conditions in the neighborhood of a Qth order fixed point. The behavior of the mapping T^Q in some neighborhood of this point is determined by the linearization of T^Q at the fixed point. Since T is a mapping of the plane, the linearized mapping is a 2×2 matrix, M;

$$\begin{pmatrix} p' - p_f \\ q' - q_f \end{pmatrix} = M \begin{pmatrix} p - p_f \\ q - q_f \end{pmatrix} , \tag{24}$$

where (p_f, q_f) are the coordinates of the Qth order fixed point. Since T is area preserving so is M; therefore

$$\det(M) = 1 . \tag{25}$$

The character of the invariant curves of the linear mapping is determined by the residue, as defined in Ref. 10:

$$R = \tfrac{1}{4} [2 - \mathrm{Tr}(M)] . \tag{26}$$

Since, from (25), the product of the eigenvalues of M is 1, knowledge of R yields the eigenvalues. Table I lists the type of fixed point as determined by R. As succinctly shown in Arnold and Avez (Appendix 27),[9] hyperbolic fixed points have real eigenvalues and thus along the eigenvectors iteration of the mapping causes exponential divergence or convergence (every fixed point in a C system is hyperbolic). Elliptic fixed points have complex conjugate eigenvalues of modulus unity so the mapping causes rotation. For the parabolic case the eigenvalues are either both +1 or −1 ($R = 0$ or 1). In this case the eigenvectors are collinear. The $R = 0$ case is special since along the eigenvector every point is a fixed point under the mapping.

TABLE I. Character of fixed point as determined by the residue.

Residue	Type of fixed point
$R > 1$	Hyperbolic with reflection
$R = 1$	Parabolic with reflection
$0 < R < 1$	Elliptic
$R = 0$	Parabolic (integrable systems)
$R < 0$	Hyperbolic

Each of the Q fixed points in a family have the same residue. If $R \neq 0$ then for each rotation number there are typically two interleaved families of fixed points: one with $R > 0$ and the other with $R < 0$. For example, if one family has $0 < R < 1$ then the mapping must have closed elliptical invariant curves in the neighborhood of the fixed points. Between each of the elliptical fixed points there will be a hyperbolic fixed point. The extensions of the eigenvectors of this point form separatricies between the elliptic points. This structure has the appearance of a chain of Q islands about the first-order fixed point (see Ref. 11). Upon discovery of such a chain it is natural to consider the rotation number of the curves which surround the Qth order fixed point. At rational values of this new rotation number there will again be higher-order fixed points which may again be elliptic or hyperbolic. For a nonintegrable system this progression of higher-order fixed points about fixed points never terminates. Thus surface of section curves, which appear to be smooth, are in reality composed of an infinite series of islands within islands and are thus not actually smooth. Following the reasoning in Sec. IV the second integral (16) would not exist.

If $R = 0$, however, there is no infinite series of islands. For this case the curve emanating from the fixed point along the eigenvector of the linear mapping is a line of fixed points. This is the only case for which a smooth curve of Qth order fixed points surrounding the central point can exist. When these curves exist the mapping is integrable. For this case it is easy to find fixed points moving out in any direction from the center. This is to be contrasted with the $R \neq 0$ case for which there are typically only $2Q$ fixed points with $\omega = P/Q$.

Computation of R is an extremely sensitive, quantitative check for integrability of the two-degree-of-freedom system, limited only by the accuracy to which the orbits can be calculated.

To compute R it is first necessary to find the higher-order fixed points. Using single precision (14 digit) arithmetic on a CDC 7600 computer we were able to determine fixed points to 11 digits of accuracy by using Newton's method to converge on a rational value of rotation number. Once the fixed point is determined the linearized mapping is computed by choosing two initial conditions in a neighborhood of and not collinear with the fixed point (explicit expressions are given in Ref. 11). We found, by varying the distance from the fixed point, that for distances less than 10^{-6} the mapping

TABLE II. Values of the residues obtained for the test-wave Hamiltonian with the parameters of Fig. 4. Initial conditions are $I_2=0.001$, $\psi_2=0.0$, $K=-0.1$ with I_1 determining the rotation number.

Rotation number	$I_1(0)$	Residue	Error
1/3	0.7338	4.0×10^{-10}	2×10^{-9}
1/5	0.8741	4.4×10^{-9}	4×10^{-8}
1/6	0.9035	6.7×10^{-9}	6×10^{-8}
1/7	0.9260	8.7×10^{-9}	8×10^{-8}
1/8	0.9444	1.1×10^{-8}	9×10^{-8}
1/9	0.9601	1.2×10^{-8}	1×10^{-7}
1/10	0.9738	1.4×10^{-8}	1×10^{-7}

was linear to integration accuracy. Using this scheme we calculated the residue for 50 fixed points on the $K=-0.1$ and $K=-0.5$ surfaces. We chose fixed points at various arbitrary angles around two elliptic first-order fixed points on a surface of section. To estimate the error of the calculation we also calculated the determinant of the matrix (25). For each of the 50 fixed points the error was always larger than $|R|$; typical values were $|R|=10^{-4}\pm10^{-3}$.

For more convincing evidence that $R=0$ everywhere, we used double-precision (28 digit) arithmetic to calculate the residue for select few fixed points. For these fixed points the integration accuracy was 17 digits and the distance to nearby points was picked as 10^{-11}. Table II shows that again the value of R was zero within numerical accuracy for each fixed point.

We conclude that not only does the surface of section consist of smooth curves on the scale visible in Fig. 4, but also to at least distances of the order of 10^{-7}. Thus to this accuracy the second integral exists.

VII. CONCLUSIONS AND SPECULATIONS

Based on the evidence of the Poincaré surface of section and Greene's method, the two-triad test-wave Hamiltonian is almost certainly integrable. The evidence of linear separation of neighboring orbits indicates integrability for up to four triads, albeit in a more qualitative way. It seems reasonable to speculate that since there seems to be nothing special about four degrees of freedom, the M-degree-of-freedom test-wave Hamiltonian may also be integrable. To jump from two to four to M degrees of freedom is hardly justified, but a major purpose of this paper is to stimulate interest in the search for integrals of motion.

It is interesting to speculate on the characteristics of the Hamiltonian (1) that are required for integrability: perhaps this Hamiltonian is a member of a more general class of integrable Hamiltonians. For example, if we compare the test-wave Hamiltonian to that of Ford and Lunsford[8]

$$H=\omega_1 J_1+\omega_2 J_2+\omega_3 J_3-\epsilon_1(J_1^2 J_2)^{1/2}\cos(2\theta_1-\theta_2)\,,$$
$$-\epsilon_2(J_1 J_2 J_3)^{1/2}\cos(\theta_1-\theta_2-\theta_3)\,, \qquad (27)$$

it appears that the essential difference is that in our Hamiltonian only one wave appears in more than one coupling term. Thus it may be possible that a Hamiltonian with a more general interaction term is also integrable, although by Siegel's theorem[5] this is not probable.

ACKNOWLEDGMENTS

The author is indebted to the Lawrence Berkeley Laboratory for the use of their computing facilities, to Nino Pereira for constructive criticism of the manuscript, and to Joseph Ford for bringing the residue method to his attention. Neil Pomphrey and Kenneth Watson were constant sources of support and guidance during this study. This research was supported by the ONR under Contract No. N00014-78-C-0050.

[1]G. Contopoulos, Astrophys. J. 138, 1297 (1963).
[2]J. Ford, S. D. Stoddard, and J. S. Turner, Prog. Theor. Phys. 50, 1547 (1973).
[3]M. Hénon, Phys. Rev. B 9, 1921 (1974).
[4]F. Calogero, C. Marchioro, and O. Ragniso, Nuovo Cimento Lett. 13, 383 (1975); J. Moser, Adv. Math. 16, 197 (1975).
[5]C. L. Siegel, Ann. Math. 42, 806 (1941); Math. Anal. 128, 144 (1954).
[6]M. Hénon and C. Heiles, Astrophys. J. 69, 73 (1964).
[7]L. J. Laslett, in Proceedings of the International Conference on High Energy Accelerators, SLAC CONF 740522, pp. 394–400 (1974) (unpublished).
[8]J. Ford and G. H. Lunsford, Phys. Rev. A 1, 59 (1970).
[9]V. I. Arnold and A. Avez, *Ergodic Problems of Classical Mechanics* (Benjamin, New York, 1968).
[10]J. M. Greene, J. Math. Phys. 9, 760 (1968).
[11]J. Ford and G. H. Lunsford, J. Math. Phys. 13, 700 (1972); J. Ford, J. Math. Phys. 13, 123 (1972).
[12]J. D. Meiss and K. M. Watson, *Topics in Nonlinear Dynamics*, edited by S. Jorna (American Institute of Physics, New York, 1978), Vol. 46, pp. 296–323.
[13]K. M. Watson, B. J. West, and B. I. Cohen, J. Fluid Mech. 77, 185 (1976).
[14]H. Wilhelmsson, and V. P. Pavlenko, Phys. Scr. 7, 213 (1973); J. Weiland and H. Wilhelmsson, *Coherent Non-Linear Interaction of Waves in Plasmas* (Pergamon, New York, 1977), pp. 121–126.
[15]R. H. Kraichnan, Phys. Fluids 6, 1603 (1963).
[16]H. Goldstein, *Classical Mechanics* (Addison-Wesley,

Reading, Mass., 1950).
[17]M. Abramowitz and I. A. Stegun, *Handbook of Mathematical Functions*, National Bureau of Standards (U. S. GPO, Washington, D.C., 1964), Chaps. 16–17.
[18]J. A. Armstrong, N. Bloembergen, J. Ducing, and P. S. Pershan, Phys. Rev. 127, 1918 (1962).
[19]L. F. McGoldrick, J. Fluid Mech. 21, 305 (1965).
[20]B. Coppi, M. N. Rosenbluth, and R. N. Sudan, Ann. Phys. 55, 207 (1969).
[21]G. Contopoulos, in *Dynamics of Stellar Systems*, edited by A. Hayli (Reidel, Boston, 1975), pp. 209–225.
[22]G. Casati and J. Ford, J. Comput. Phys. 20, 97 (1976).